Biophysical Journal

Supporting Material

Katanin Severing and Binding Microtubules Are Inhibited by Tubulin Carboxy Tails

Megan E. Bailey,[1,2] Dan L. Sackett,[3] and Jennifer L. Ross[2,*]

[1]Molecular and Cellular Biology Graduate Program and [2]Department of Physics, University of Massachusetts-Amherst, Amherst, Massachusetts; and [3]Program in Physical Biology, Eunice Kennedy Shriver National Institute of Child Health and Human Development, National Institutes of Health, Bethesda, Maryland

Supplemental Table 1: Fits for data in Figure 1

Microtubules Alone, fit equation: $I(t) = I_0\left(1 - t/\tau\right)$ (Eq. 3)					
$I_0 = 1.012 \pm 0.002$	$\tau = 3400 \pm 100$ s			$\chi^2 = 0.0073$	$R^2 = 0.93$
MTs + Xl-p60, fit equation: $I(t) = I_0 \exp\left(-t/\tau\right)$ (Eq. 1)					
$I_0 = 1.25 \pm 0.04$	$\tau = 62 \pm 2$ s			$\chi^2 = 0.30$	$R^2 = 0.95$
MTs + GFP-Hu-p60, fit equation: $I(t) = I_0 \exp\left(-t/\tau\right) + I_\infty$ (Eq. 2)					
$I_0 = 0.99 \pm 0.03$	$\tau = 66 \pm 3$ s	$I_\infty = 0.099 \pm 0.008$		$\chi^2 = 0.18$	$R^2 = 0.95$

Supplemental Table 2: Fits for data in Figure 2

Exponential Growth Phase (i) Binding Rates fit equation: $I(t) = A\exp\left(t/\tau_{bind}\right)$ (Eq 4)

Concentration of Hu-p60	A	τ_{bind} (s)	χ^2	R^2
50 nM	0.34 ± 0.01	6.3 ± 0.2	28	0.80
100 nM	0.084 ± 0.010	3.0 ± 0.2	15	0.72
200 nM	0.18 ± 0.01	3.32 ± 0.10	20	0.87
300 nM	0.117 ± 0.007	2.56 ± 0.07	5.9	0.87
400 nM	0.115 ± 0.007	1.84 ± 0.05	2.6	0.92
500 nM	0.029 ± 0.003	1.10 ± 0.03	1.4	0.91

Constant phase (ii), Average and Standard Deviation

Concentration of Hu-p60	Average	Standard Deviation
50 nM	1.80	0.04
100 nM	2.35	0.04
200 nM	3.19	0.04
300 nM	2.79	0.05
400 nM	3.16	0.14
500 nM	1.86	0.06

Exponential Decay Phase (iii) Severing Rates fit equation: $I(t) = \exp\left(-\frac{t-t_0}{\tau_{sever}}\right)$ (Eq 5)

Concentration of Hu-p60	t_0	τ_{sever}	χ^2	R^2
50 nM	43.66 ± 0.03	16.97 ± 0.06	2.7	0.990
100 nM	36.18 ± 0.02	16.55 ± 0.05	1.2	0.995
200 nM	34.60 ± 0.02	7.95 ± 0.03	1.3	0.995
300 nM	28.55 ± 0.01	6.64 ± 0.02	0.99	0.995
400 nM	26.19 ± 0.02	6.05 ± 0.02	1.4	0.995
500 nM	20.29 ± 0.03	8.05 ± 0.06	2.1	0.981

Association Rate fit equation: $r([p60]) = k_{on}[p60]$ (Eq 6)

k_{on} = 0.0016 ± 0.0002 1/(M-s)	χ^2 = 0.07	R^2 = 0.80

Maximum Intensity Binding fit equation: $I([p60]) = I_{max}\frac{[p60]}{K_D + [p60]}$ (Eq 7)

I_{max} = 3.5 ± 0.3	K_D = 45 ± 20 nM	χ^2 = 0.18	R^2 = 0.87

Severing Rate fit equation: $k\left([p60]\right) = k_{max}\frac{[p60]}{K_M + [p60]}$ (Eq 8)

k_{max} = 0.19 ± 0.04	K_M = 130 ± 80 nM	χ^2 = 0.0021	R^2 = 0.79

Oligomerization Rate, Constant Phase (ii) fit equation: $r([p60]) = r_0 + k_{olig}[p60]$ (Eq 9)

r_0 = 0.017 ± 0.002 1/s	k_{olig} = 0.000052 ± 0.000007 1/(nM-s)	χ^2 = 2.9 x 10^{-5}	R^2 = 0.94

Supplemental Table 3: Fits for data in Figure 3

Microtubules alone: $I(t)=I_0\left(1-{}^{t}/_{\tau}\right)$					
$I_0 = 1.0 \pm 0.4$	$\tau = 10^{20}$ s			$\chi^2 = 0.14$	$R^2 = 0.08$
Microtubules + p60, fit equation: $I(t)=I_0\exp\left(-{}^{t}/_{\tau}\right)+I_\infty$					
$I_0 = 0.73 \pm 0.02$	$\tau = 47 \pm 2$ s	$I_\infty = 0.106 \pm 0.007$		$\chi^2 = 0.15$	$R^2 = 0.97$
Microtubules + p60 + 50 nM tubulin, fit equation: $I(t)=I_0\exp\left(-{}^{t}/_{\tau}\right)+I_\infty$					
$I_0 = 0.57 \pm 0.02$	$\tau = 270 \pm 19$ s	$I_\infty = 0.43 \pm 0.02$		$\chi^2 = 0.015$	$R^2 = 0.99$
Microtubules + p60 + 500 nM tubulin, fit equation: $I(t)=I_0\left(1-{}^{t}/_{\tau}\right)$					
$I_0 = 1.053 \pm 0.007$	$\tau = 5000 \pm 600$ s			$\chi^2 = 0.064$	$R^2 = 0.43$
Microtubules + p60 + 1 μM tubulin, fit equation: $I(t)=I_0\exp\left(-{}^{t}/_{\tau}\right)+I_\infty$					
$I_0 = 0.3 \pm 0.2$	$\tau = 1100 \pm 800$ s	$I_\infty = 0.6 \pm 0.2$		$\chi^2 = 0.0063$	$R^2 = 0.92$
Microtubules + p60 + 6 μM tubulin, fit equation: $I(t)=I_0\exp\left(-{}^{t}/_{\tau}\right)+I_\infty$					
$I_0 = 0.150 \pm 0.005$	$\tau = 170 \pm 20$ s	$I_\infty = 0.879 \pm 0.006$		$\chi^2 = 0.007$	$R^2 = 0.92$
Microtubules + p60 + 10 μM tubulin, fit equation: $I(t)=I_0\left(1-{}^{t}/_{\tau}\right)$					
$I_0 = 0.993 \pm 0.003$	$\tau = 5100 \pm 300$ s			$\chi^2 = 0.012$	$R^2 = 0.78$
Maximum GFP-Katanin Intensity, fit equation: $c[tub]=c_0\left(\frac{1}{1+\left({}^{[tub]}/_{K_{D,app}}\right)^n}\right)$ (Eq 10)					
$c_0 = 4.6 \pm 0.1$ nM	$n = 0.80 \pm 0.05$		$K_{D,app} = 90 \pm 10$ nM	$\chi^2 = 0.029$	$R^2 = 0.998$

Supplemental Table 4: Fits for data in Figure 4

Microtubules + p60, fit equation: $I(t)=I_0\left(1-{t}/{\tau}\right)$					
I_0 = 1.256 ± 0.008	τ = 1310 ± 80 s			χ^2 = 0.17	R^2 = 0.69
Microtubules + p60 + 50 nM tubulin, fit equation: $I(t)=I_0\exp\left(-{t}/{\tau}\right)+I_\infty$					
I_0 = 1.44 ± 0.02	τ = 59 ± 2 s	I_∞ = 0.471 ± 0.008		χ^2 = 0.083	R^2 = 0.99
Microtubules + p60 + 500 nM tubulin, fit equation: $I(t)=I_0\exp\left(-{t}/{\tau}\right)+I_\infty$					
I_0 = 0.70 ± 0.02	τ = 58 ± 3 s	I_∞ = 0.392 ± 0.008		χ^2 = 0.081	R^2 = 0.96
Microtubules + p60 + 1 µM tubulin, fit equation: $I(t)=I_0\exp\left(-{t}/{\tau}\right)+I_\infty$					
I_0 = 0.90 ± 0.02	τ = 43 ± 1 s	I_∞ = 0.210 ± 0.005		χ^2 = 0.066	R^2 = 0.98
Microtubules + p60 + 6 µM tubulin, fit equation: $I(t)=I_0\exp\left(-{t}/{\tau}\right)+I_\infty$					
I_0 = 0.98 ± 0.02	τ = 45 ± 1 s	I_∞ = 0.104 ± 0.004		χ^2 = 0.45	R^2 = 0.99
Microtubules + p60 + 10 µM tubulin, fit equation: $I(t)=I_0\exp\left(-{t}/{\tau}\right)+I_\infty$					
I_0 = 2.34 ± 0.02	τ = 31.7 ± 0.4 s	I_∞ = 0.012 ± 0.003		χ^2 = 0.031	R^2 = 0.997
Characteristic Decay Rate, fit equation: $r([tub])=r_0+k_{replace,tub}[tub]$ (Eq 10)					
r_0 = 0.018 ± 0.002 (1/s)	k_{off} = 0.00000120 ± 0.0000004 (1/nM-s)			χ^2 = 3.3 x 10^{-5}	R^2 = 0.77
Final GFP-Katanin Intensity, fit equation: $c[tub]=c_0\left(\frac{1}{1+\left({[tub]}/{K_{D,app}}\right)^n}\right)$					
c_0 = 1.08 ± 0.09 s	$K_{D,app}$ = 40 ± 30 nM	n = 0.4 ± 0.1		χ^2 = 0.22	R^2 = 0.97

Supplemental Table 5: Fits for data in Figure 5

Microtubules alone, fit equation: $I(t)=I_0\left(1-{t}/{\tau}\right)$					
$I_0 = 0.992 \pm 0.002$	$\tau = 18000 \pm 2000$ s			$\chi^2 = 0.0051$	$R^2 = 0.40$
Microtubules + p60, fit equation: $I(t)=I_0\exp\left(-{t}/{\tau}\right)+I_\infty$					
$I_0 = 1.43 \pm 0.03$	$\tau = 37.0 \pm 0.7$ s	$I_\infty = 0.051 \pm 0.002$		$\chi^2 = 0.022$	$R^2 = 0.993$
Microtubules + p60 + 50 nM tubulin, fit equation: $I(t)=I_0\exp\left(-{t}/{\tau}\right)+I_\infty$					
$I_0 = 0.40 \pm 0.01$	$\tau = 71 \pm 4$ s	$I_\infty = 0.743 \pm 0.004$		$\chi^2 = 0.0049$	$R^2 = 0.98$
Microtubules + p60 + 50 nM tubulin denatured tubulin, fit equation: $I(t)=I_0\exp\left(-{t}/{\tau}\right)+I_\infty$					
$I_0 = 0.26 \pm 0.05$	$\tau = 500 \pm 200$ s	$I_\infty = 0.78 \pm 0.05$		$\chi^2 = 0.009$	$R^2 = 0.94$
Microtubules + p60 + 50 nM tubulin denatured subtilisin-treated tubulin, fit equation: $I(t)=I_0\exp\left(-{t}/{\tau}\right)+I_\infty$					
$I_0 = 2.40 \pm 0.09$	$\tau = 42 \pm 1$ s	$I_\infty = 0.149 \pm 0.003$		$\chi^2 = 0.016$	$R^2 = 0.992$

Supplemental Table 6: Fits for data in Figure 6

Microtubules alone, fit equation: $I(t) = I_0\left(1 - t/\tau\right)$					
I_0 = 0.992 ± 0.002	τ = 18000 ± 2000 s			χ^2 = 0.0051	R^2 = 0.40
Microtubules + p60, fit equation: $I(t) = I_0 \exp\left(-t/\tau\right) + I_\infty$					
I_0 = 1.43 ± 0.03	τ = 37.0 ± 0.7 s	I_∞ = 0.051 ± 0.002		χ^2 = 0.022	R^2 = 0.993
Microtubules + p60 + 50 nM tubulin, fit equation: $I(t) = I_0 \exp\left(-t/\tau\right) + I_\infty$					
I_0 = 0.40 ± 0.01	τ = 71 ± 4 s	I_∞ = 0.743 ± 0.004		χ^2 = 0.0049	R^2 = 0.98
Microtubules + p60 + 50 nM βCTT-BSA, fit equation: $I(t) = I_0 \exp\left(-t/\tau\right) + I_\infty$					
I_0 = 0.142 ± 0.004	τ = 160 ± 13 s	I_∞ = 0.853 ± 0.004		χ^2 = 0.006	R^2 = 0.95
Microtubules + p60 + 50 nM αCTT-BSA, fit equation: $I(t) = I_0 \exp\left(-t/\tau\right) + I_\infty$					
I_0 = 0.50 ± 0.01	τ = 93 ± 4 s	I_∞ = 0.630 ± 0.004		χ^2 = 0.017	R^2 = 0.98
Microtubules + p60 + 50 nM ΔY-αCTT-BSA, fit equation: $I(t) = I_0 \exp\left(-t/\tau\right) + I_\infty$					
I_0 = 0.90 ± 0.04	τ = 49 ± 2 s	I_∞ = 0.537 ± 0.002		χ^2 = 0.015	R^2 = 0.98

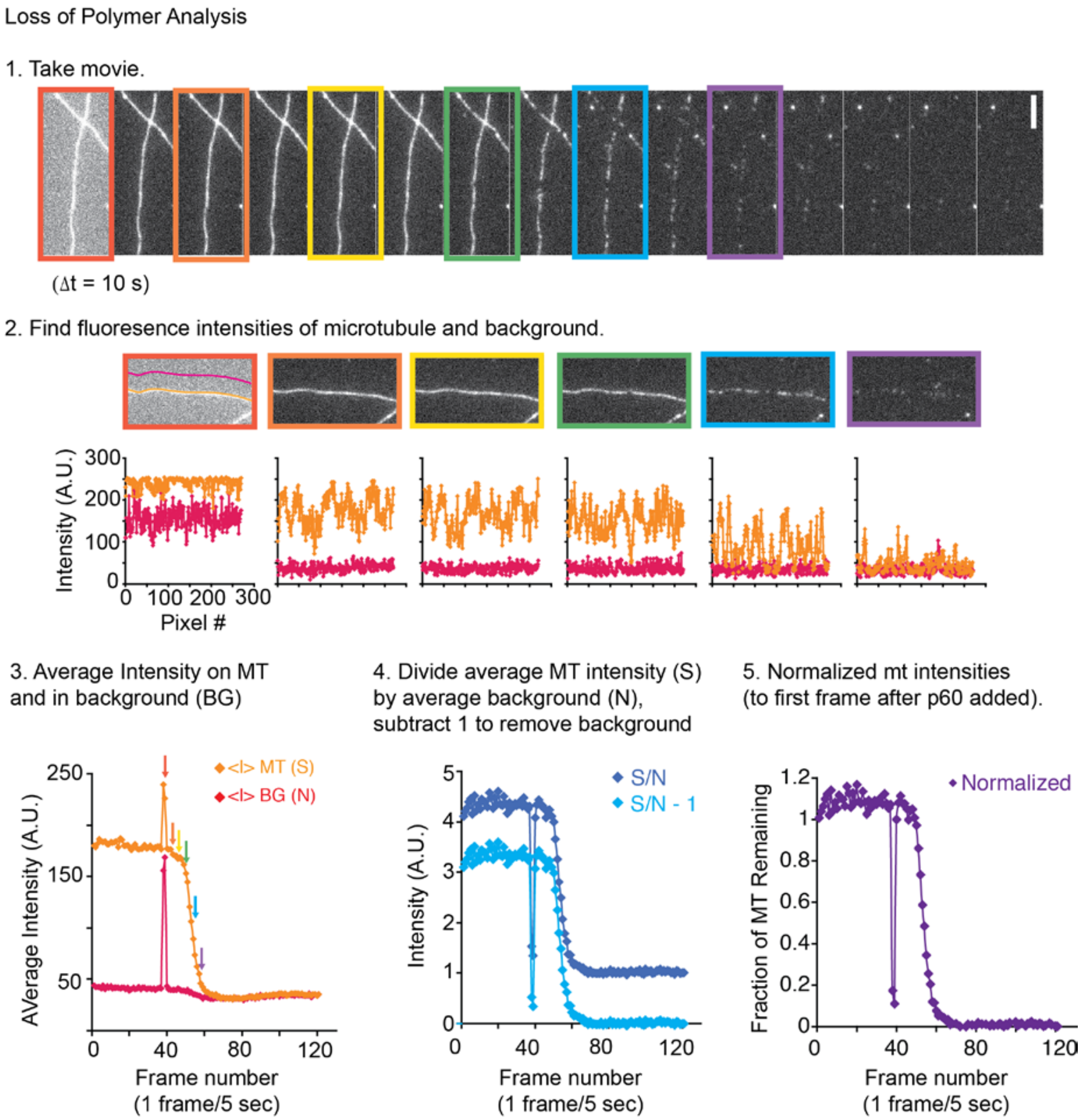

Supplemental Figure 1 Example displaying how we analyzed data step-by-step. (1) We took a movie of the microtubule over time. Outlined images are shown as examples. (2) For each image, we measured the average intensity along the length of the filament and in the background near the filament. We show the intensity along the length of the microtubule, and we took the average of these traces over the length of the filament. (3) The average intensity of the microtubule (red diamonds, signal) and background (orange diamonds, noise) are shown for one microtubule. The arrows denote the average intensity for the matching color outlined frames. (4) Using the microtubule intensity (S) divided by the intensity on the background (N) gives the ratio of signal to noise (dark blue diamonds). We then subtracted one from this measure (light blue diamonds) to subtract the background. (5) Finally, we normalized each data set so that the data before the katanin is added is on average one. We did this by dividing the data by the intensity of the microtubule before katanin was added. After analyzing individual microtubules this way, we averaged the data from different microtubules together to give an average signal and to find the standard error to give the uncertainty.

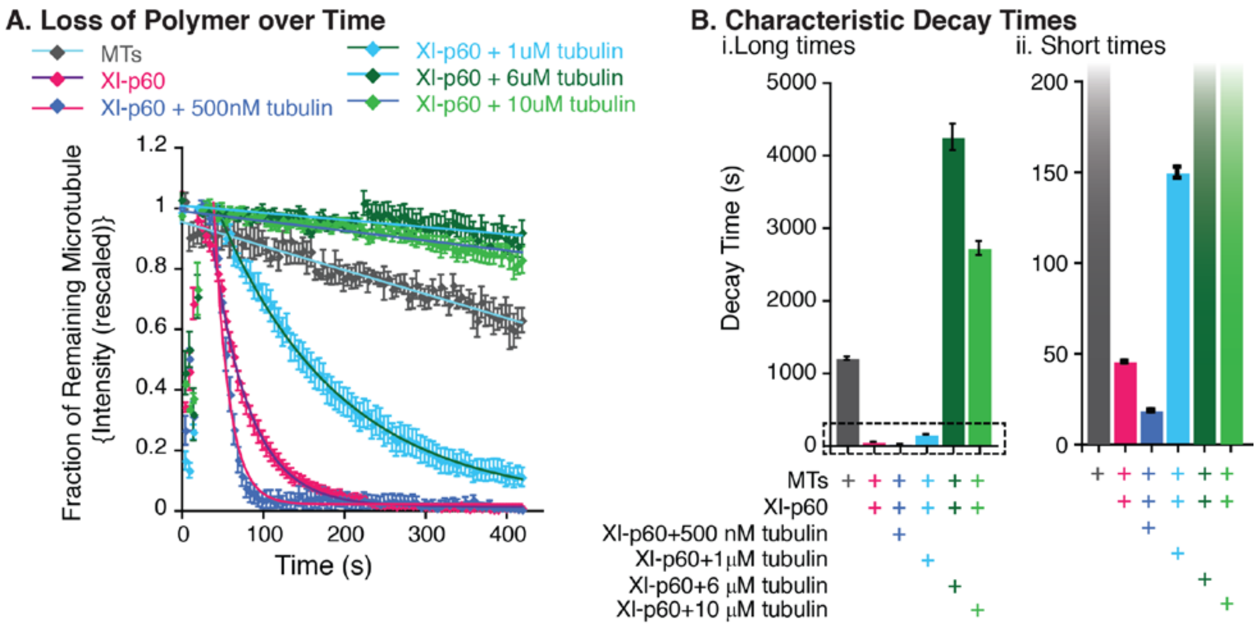

Supplemental Figure 2. Xl-p60 is inhibited by free tubulin dimers. (A) Plot of the fraction of microtubule remaining for Xl-p60 in the presence of increasing amounts of free tubulin. Error bars represent the S.E.M. (B) Plot of the characteristic decay times from fit to data in part A. (i) All decay times for all data sets. (ii) Zoom in of data from part I to facilitate visualization of the fast decay times. Error bars represent the uncertainty from the fits. For the data shown, the numbers of microtubules analyzed were: microtubules alone (N = 4), microtubules with 10 µM tubulin (N = 10), microtubules with Xl-p60 (N = 55), microtubules with Xl-p60 and 500 nM free tubulin (N = 17), microtubules with Xl-p60 and 1 µM free tubulin (N=14), microtubules with Xl-p60 and 6 µM free tubulin (N = 10), microtubules with Xl-p60 and 10 µM free tubulin (N = 15).

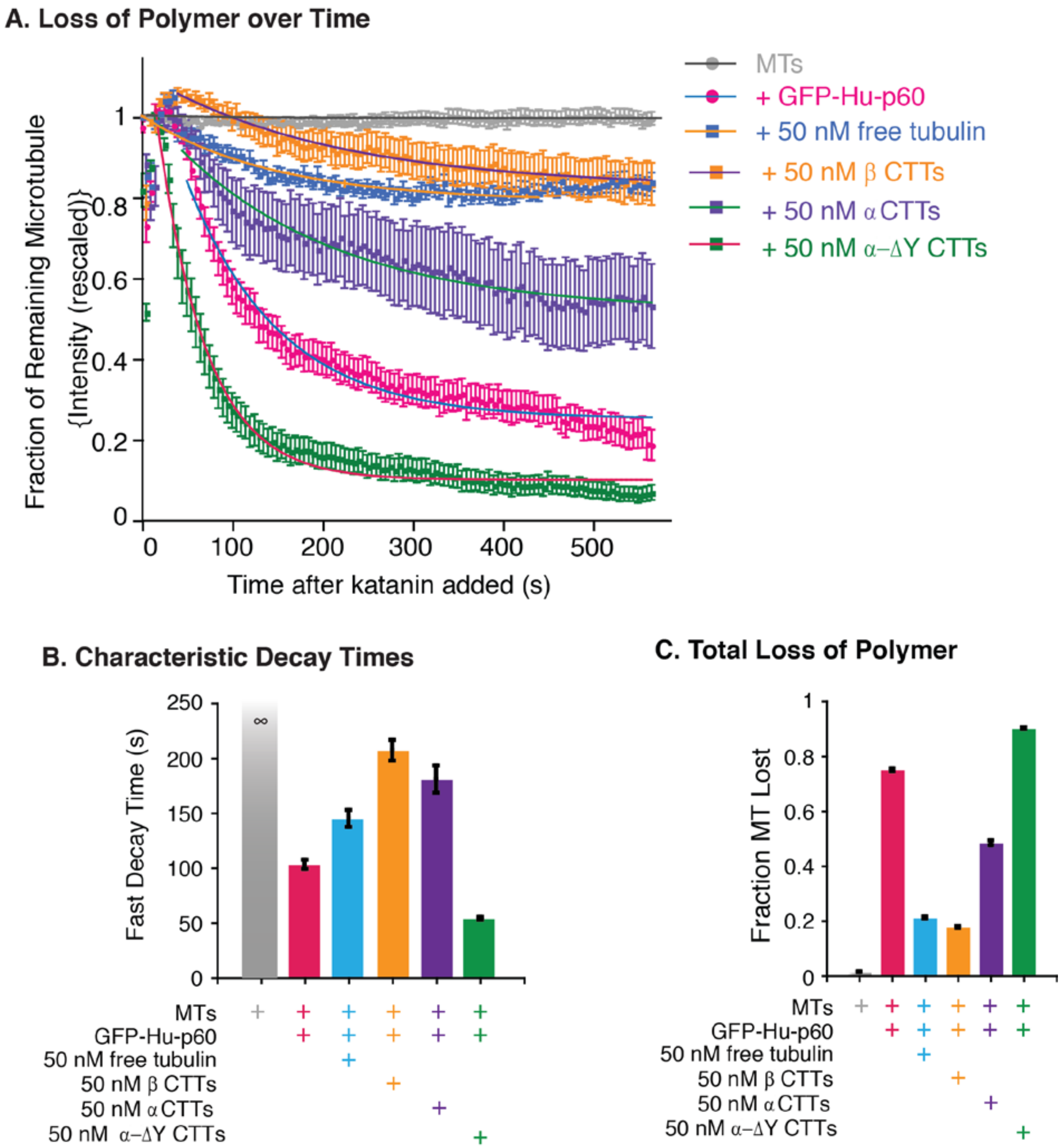

Supplemental Figure 3 Carboxy-terminal tails of beta, alpha, and detyrosinated alpha tubulin without BSA also inhibit microtubule severing by GFP-Hu-p60. (A) Plot of the fraction of microtubule remaining for GFP-Hu-p60 in the presence of increasing amounts of free tubulin. Data was fit to equation 2. Error bars represent the S.E.M. (B) Plot of the characteristic decay times determined from the exponential decay fits to the data in part A. Error bars represent the uncertainty from the fits. (C) The total loss of polymer was determined from the long-time asymptote from the fits to the data in part A. The error bars represent the uncertainty of the fit parameters. For the data shown, the numbers of microtubules analyzed were: microtubules alone (N = 28), microtubules with GFP-Hu-p60 (N = 29), microtubules with 100 nM GFP-Hu-p60 and 50 nM free tubulin (N = 24), microtubules with GFP-Hu-p60 and 50 nM beta CTTs (N=30), microtubules with GFP-Hu-p60 and 50 nM alpha CTTs (N = 27), microtubules with GFP-Hu-p60 and 50 nM detyrosinated alpha CTTs (N = 37).